Magnetic field measurement on ^{87}Rb atomic fountain clock

Chunyan Shi (史春艳), Rong Wei (魏 荣)*, Zichao Zhou (周子超), Desheng Lü (吕德胜), Tang Li (李 唐), and Yuzhu Wang (王育竹)**

Key Laboratory of Quantum Optics, Shanghai Institute of Optics and Fine Mechanics, Chinese Academy of Sciences, Shanghai 201800, China

**E-mail: weirong@siom.ac.cn; **e-mail: yzwang@mail.shcnc.ac.cn*

Received September 22, 2009

An experiment on measuring the magnetic field in Ramsey interaction region of the atomic fountain clock by detecting the Zeeman frequency shift of ^{87}Rb hyperfine transition is presented. By mu-metal shielding and coils compensating, the magnetic fluctuations resulting from asymmetry and instability are less than 10 and 0.025 nT, respectively. The relative frequency uncertainty of atomic fountain clock caused by the magnetic field is less than 5.4×10^{-16}.

OCIS codes: 020.7490, 120.2650, 120.3940.

doi: 10.3788/COL20100806.0549.

Atomic fountain clocks (AFCs) are the most accurate clocks in the International Atomic Time (TAI, Temps Atomique International) system. Its frequency uncertainty has reached 10^{-16}[1]. At present, about 30 AFCs are running at various laboratories all over the world, and more AFCs are being studied, including a research being conducted into a ^{87}Rb AFC by our group at the Shanghai Institute of Optics and Fine Mechanics (SIOM). The project began in 2005 and is estimating uncertainty at present. Typically, the uncertainty of fountain clocks is firstly estimated by systematic (type B) uncertainties[2] and then by TAI comparing. In a fountain clock, the frequency-shifting physical theories are very similar to those in a conventional cesium beam clock[1,3]. Detailed descriptions of these effects can be found in Refs. [4–6]. As magnetic field affects the uncertainty of an atomic clock through the second-order Zeeman effect and the Majorana transition, the evaluation of the magnetic field is very important to the frequency uncertainty of AFC. Most atomic fountains, such as USA-NIST-F1, generate their magnetic field maps by measuring the transition frequency of magnetically sensitive transition between sublevels of the same hyperfine level using a low-frequency excitation coil transverse to the fight path[7], which requires coils and probably produces additional electromagnetic noise. Our fountain clock field map is produced by measuring magnetically sensitive transitions between two hyperfine levels by spatial microwave coupling. In this way, the low-frequency excitation coil is not required.

The ^{87}Rb ground state hyperfine structure is shown in Fig. 1. When the magnetic field is weak, $\Delta v_{\text{Zeeman1}}$ and $\Delta v_{\text{Zeeman2}}$, the first-order and second-order Zeeman shifts brought by σ transition between ^{87}Rb Zeeman hyperfine energy levels ($\Delta F_{\text{g}} = \pm1, \Delta m_F = 0$) (the subscrip "g" represents ground state) can be described as

$$\Delta v_{\text{Zeeman1}} = k_1 m_F H_c, \tag{1}$$

$$\Delta v_{\text{Zeeman2}} = k_2(1 - m_F^2)\overline{H_c^2}, \tag{2}$$

where $k_1 = 1.401952\times10^6$ Hz/Gs and $k_2 = 5.751460\times10^2$ Hz/Gs^2[8–10] are the first-order and second-order Zeeman coefficients, respectively, m_F is the magnetic quantum number, H_c is the magnetic intensity in Ramsey interaction region, and $\overline{H_c^2}$ is the time-average of the square of the magnetic intensity applied to atoms when they fly in Ramsey interaction region. For clock transition ($F = 1, m_F = 0 \rightarrow F = 2, m_F = 0$) of ^{87}Rb, the first-order Zeeman shift equals 0, and the relative frequency uncertainty brought by the second-order Zeeman shift can be expressed as[8,10]

$$\sigma_{\text{Zeeman}} = \frac{\delta v_{\text{Zeeman}}}{\nu_0} = 2k_2 \frac{\overline{H_c^2}}{\nu_0} \frac{\delta H}{\overline{H_c}}, \tag{3}$$

where ν_0 is the clock frequency, $\overline{H_c}$ is the average magnetic intensity in Ramsey interaction region, δH is the fluctuation of H_c, which includes two parts, one is the time instability of magnetic intensity $\overline{H_c}$ mainly coming from current fluctuation of orientation magnetic field coils, and the other is spatial asymmetry of C-field which turns the error of launching height of atoms to the error of Zeeman effect. Equation (3) indicates that reducing H_c can decrease σ_{Zeeman}, but reducing H_c will increase the frequency uncertainty caused by the Majorana transition[11], which occurs when an atom passes through a weak inhomogeneous magnetic field in the flight region. Following Ref. [1], the atomic fountain research shows that when δH is limited in several nanoteslas and H_c is about 100 nT, the uncertainty caused by Majorana transition is estimated to be below 10^{-16}.

Figure 2 illustrates the mechanical design of the fountain. One cycle of the fountain process is described as follows: ^{87}Rb atoms are trapped and cooled by a

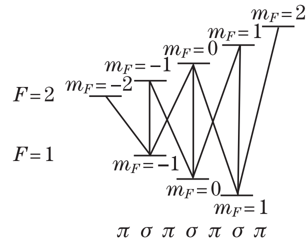

Fig. 1. ^{87}Rb ground state hyperfine.

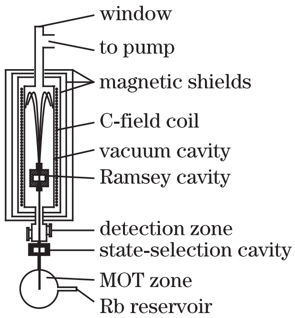

Fig. 2. Setup of the fountain clock at SIOM.

magneto-optical trap (MOT) from rubidium background gas at the MOT zone with a loading time of 1000 ms, then further cooled to 4 μK by optical molasses (OM) in 100 ms. After moving molasses stage, cold atoms in states of $F = 2$ are launched at a velocity of 4.188 m/s, passing through the state-selection cavity and detection zone, and then are distributed at the atomic substate of $F = 1, m_F = 0$, reaching the Ramsey interaction region through which the atoms pass and interact with microwave $\pi/2$ pulse twice, once on their way up and again on their way down. When the falling atoms pass through the first transverse standing-wave light field of detection zone tuned to the $F_{\rm g} = 2 \rightarrow F_{\rm e} = 3$ transition (subscripts "g" and "e" denote ground state and excitation state, respectively), the fluorescence photons of $F_{\rm g} = 2$ atoms are detected by a photodiode, then these atoms are pushed away by a traveling wave field. The others (i.e., atoms of $F_{\rm g} = 1$) are pumped to $F_{\rm g} = 2$ by a second transverse standing-wave light field of detection zone tuned to the $F_{\rm g} = 1 \rightarrow F_{\rm e} = 2$ transition. When the atoms pass through the third transverse standing-wave light field, which are tuned to $F_{\rm g} = 2 \rightarrow F_{\rm e} = 3$, the fluorescence photons are detected by a photodiode, and then the time-of-flight (TOF) signals are fed into computer.

To make the magnetic field of the interaction region meet the requirement of AFC, three layers of mu-metal shields and one layer of soft iron magnetic shield are added to the surrounding interacting region to attenuate the earth magnetic field and other residual magnetic fields. A solenoid, with a pair of magnetic field compensation coils and a pair of magnetic shielding compensation coils set at its two ends, is used to generate the mean C-field along the interaction region.

The magnetic intensity and its asymmetry in the Ramsey interaction region (from 57 to 90 cm) is directly measured by a magnetometer before assemblage. The result indicates that the magnetic fluctuation in the region is less than 2 nT. As many factors affect the effect of the magnetic shielding, the intensity should be evaluated when it is operating. At this time, it cannot be detected by the magnetometer directly; instead, we measure the Zeeman sublevel split of atoms induced by the magnetic field. According to Eq. (1), the magnetic field in the interaction zone can be worked out. Both time instability and spatial asymmetry of the magnetic field can affect the accuracy of the fountain. As spatial asymmetry is mainly caused by the fluctuation of the C-field current, it is measured after the instability of the C-field is detected.

The magnetic fields in the microwave cavity and at the apogee of the atomic ballistic flight are measured. When detecting the magnetic field in a microwave cavity, microwave is fed by this TE_{011} cylindrical cavity; the microwave power is fixed to make the atomic phase change π after their interaction. The microwave frequency is then scanned and the transition probability of magnetic sublevels is acquired by detecting the fluorescence signal. Every peak of transition is fitted by Gaussian function to reduce the error caused by step-scanning. To eliminate the first-order Doppler frequency shift effect, the frequencies of the two σ transitions are subtracted. Finally, the magnetic strength in the cavity is calculated.

For measuring the magnetic field at apogee, the microwave, coupled into the vacuum chamber by an antenna placed horizontally at the top window of the chamber, is turned on when the atoms are at apogee. The curve of the transition probability followed with frequency detuning is also detected. The peak value of the two π transitions is acquired by Gaussian fitting, and the magnetic strength of the free-flight region is worked out according to

$$v_{(2,1)\rightarrow(1,0)} - v_{(2,0)\rightarrow(1,-1)} \approx 1.401952 \times 10^6 H_c. \quad (4)$$

The curves of magnetic intensity following the current of the solenoid are shown in Fig. 3, which approach a linear relationship. Two slopes are acquired by linearly fitting the points, and the average slope is then calculated as 310.8 nT/mA. Long-term detection on the current of the solenoid is shown in Fig. 4, where the current fluctuation is less than 0.015%, and the magnetic fluctuation is less than 0.02 nT.

Compared with its symmetry, the time instability can be ignored so that we can measure the magnetic field of the interaction zone much easier. When the microwave

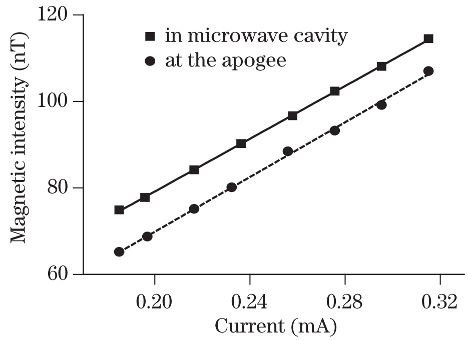

Fig. 3. Relationship between C-field intensity and its current.

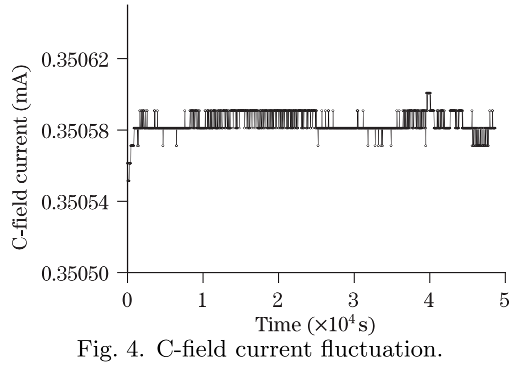

Fig. 4. C-field current fluctuation.

is coupled into the cavity, the direction of its magnetic component is parallel to the C-field. Three σ transitions can then be obtained by scanning the microwave frequency, as shown in Fig. 5. The magnetic strength is 169.7 nT in the microwave cavity according to Eq. (1), increasing the C-field current is to restrain the Majorana transition and interaction between microwave and horizontal magnetic field, its magnetic fluctuation caused by current is less than 0.025 nT.

When measuring the magnetic intensity of some position in the free-flight region, a microwave pulse of 20 ms is fed into the region when cold atoms pass through the corresponding zone. The direction of the microwave field's magnetic component is perpendicular to the C-field, and the π transition probability is higher than the σ transition probability. Figure 6 illustrates the magnetic sublevel when the microwave is turned on at 410 ms. The relationship between launch height and magnetic strength in the free-flight region is shown in Fig. 7. It is observed that the magnetic field, whose average strength is 154.1 nT and fluctuation is less than 10 nT, is enhanced as the launch height rises. The fluctuation is a little larger than the results obtained by other groups[1−3], and it is expected to be reduced to 4 nT by optimizing the currents of compensation coils.

Compared with the magnetic field reduction as the launch height declined in the free-flight region, the magnetic strength in the microwave cavity is 15.6 nT larger than the average magnetic strength in free-flight region. This result is different from that before assemblage.

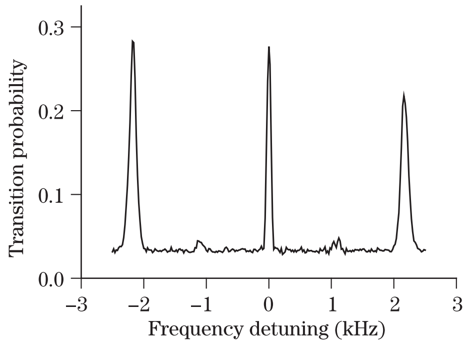

Fig. 5. Relationship between ^{87}Rb magnetic sublevel transition probability in the microwave cavity and resonator detuning.

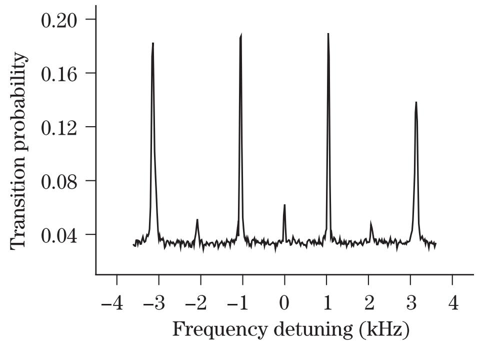

Fig. 6. Relationship between ^{87}Rb magnetic sublevel transition probability in the free-flight region and resonator detuning.

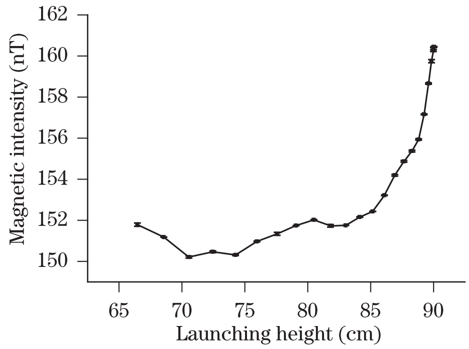

Fig. 7. Relationship between launch height and magnetic intensity in the free-flight region.

Another experiment is done to validate it. All the C-field and its compensation coils currents are reversed, and the magnetic field both in the middle and at the top of the free-flight region and in the microwave cavity is detected. It is found that the magnetic field in the free-flight region reduces, while its strength in the microwave cavity decreases when the launch height increases. A stable magnetic field is proved to be near the microwave cavity, which seriously affects the system. At present, we are trying to eliminate it.

The frequency shift and uncertainty caused by the second-order Zeeman effect of the AFC can be evaluated according to Fig. 7. Following Eq. (2), the relative frequency shift is 201.0×10^{-15}. According to Eq. (3), the fluctuation of magnetic intensity is affected mainly by two factors. One is the fluctuation of current, which is less than 0.015%, affecting 0.025 nT in magnetic field, hence contributing less than 6.5×10^{-17} to the relative frequency uncertainty of AFC. The other is the fluctuation of launch height, its apogee is 90.0 cm, its fluctuation is 0.05 cm, and the intensity of magnetic field can be linearly fitted with the error less than 0.6 nT, so its relative frequency uncertainty is less than 4.7×10^{-16}. As these two factors are uncorrelated, the total frequency uncertainty due to magnetic intensity fluctuation is less than 5.4×10^{-16}.

In conclusion, the evaluation of magnetic intensity of Ramsey region is an important work for AFC, which is obtained by measuring the transition frequencies of sub-magnetic level at SIOM. Microwave is coupled to cavity by waveguide and to free-flying region by antenna, which is simpler than the way of using low-frequency excitation coil. The intensity of orientation C-field is set to 154.1 nT by adjusting the currents of coils, and its asymmetry and instability are less than 10 and 0.025 nT, respectively, the former is expected to decrease to 4 nT by optimizing the current of coils. The second-order Zeeman frequency shift is evaluated as 201.0×10^{-15} and its uncertainty is less than 5.4×10^{-16} in the atomic fountain. These results fit the requirement of an AFC with an uncertainty of better than 1×10^{-15}.

This work was supported by the National Basic Research Program of China (No. 2005CB724506), the National Natural Science Foundation of China (Nos. 10604058 and 10974215), and the Open Research Fund of State Key Laboratory of Precision Spectroscope.

References

1. R. Wynands and S. Weyers, Metrologia **42,** S64 (2005).
2. B. Guinot and E. F. Arias, Metrologia **42,** S20 (2005).
3. J. Vanier and C. Audoin, Metrologia **42,** S31 (2005).
4. J. Vanier and C. Audoin, *The Quantum Physics of Atomic Frequency Standards* (Adam Hilger, Bristol, 1989).
5. G. Wang, W. Ji, J. Ma, L. Wang, L. Xiao, and S. Jia, Chinese J. Lasers (in Chinese) **35,** 221 (2008).
6. L. Yi, X. Qi, W. Chen, D. Zhou, T. Zhou, X. Zhou, and X. Chen, Chin. Opt. Lett. **7,** 36 (2009).
7. S. R. Jefferts, J. Shirley, T. E. Parker, T. P. Heavner, D. M. Meekhof, C. Nelson, F. Levi, G. Costanzo, A. De Marchi, R. Drullinger, L. Hollberg, W. D. Lee, and F. L. Walls, Metrologia **39,** 321 (2002).
8. Y. Wang Q. Wang, J. Fu, and T. Dong, *The Principle of Quantum Frequency Standards* (in Chinese) (Science Press, Beijing, 1986).
9. A. Daniel and Steck, "Rubidium 87 D Line Data", http://steck.us/alkalidata (September 1, 2008).
10. R. Wei, "Design and prior work of a compact rubidium atomic fountain" PhD. Thesis (in Chinese) (Shanghai Institute of Optics and Fine Mechanics, Chinese Academy of Sciences, Shanghai, 2003).
11. N. E. Majorana, Il Nuovo Cimento (in Italian) **9,** 43 (1932).